Using the CFD Technique to Analyze Tire Tread Hydroplaning Effects

Min-Feng Sung*, Chin-Fu Chen, Chao-Jung Chen
Kenda Rubber IND. CO., LTD,
No.146, Sec. 1, Chung Shan Rd., Yuanlin, Chungha 51064, Taiwan.

Corresponding author's email: bigeyes [AT] kenda.com.tw

ABSTRACT---- ***Hydroplaning is a major cause of wet-road accidents. The main contact element between the ground and vehicle is the tire. Tire safety and performance are therefore critically important. Wet roads present several uncontrollable factors. This paper uses CFD (Computational Fluid Dynamics) to analyze wet road hydroplaning effects. Fluid dynamics cannot be easily measured using normal experiments. Therefore the braking distance and record rolling vary by encoder. We propose another method to analysis it. By this result, the large groove and tire depth can reduce hydroplaning effects. A second method is modifying the tire void pattern which can reduce the hydroplaning extent by 29%.***

Keywords--- Tire, CFD, Hydroplaning.

1. INTRODUCTION

Recent developments in high technologies, new materials and advanced manufacturing methods in the motor vehicle industry have transformed the modern automobile into a universal transport. This popularity has also led lot traffic accidents, especially in winter. Active safety systems such as Electronic Stability Control (ESC) have considerably increased traffic safety. [1] Strandroth et al. [2] published an article investigating the performance of passenger cars with or without ESC systems in winter. This study examines the effects of studded tires in fatal crashes on roads covered with ice or snow in Sweden. The main study results showed that 64% of fatal crashes on roads covered with ice or snow involved loss-of-control (LOC) as a major component. More than 82% of LOC occurred due to over-steering. Tuononen et al. [3] published a paper that pointed out how to measure the tires contact length on wet-roads. Their results showed the tire contact length on dry roads was very stable, while the tire contact length became very unstable on wet roads. The tire groove function is help remove water film from the tire contact surface on wet-roads. However, when the water-film thickness becomes higher than groove's depth, hydroplaning effects will occur. In 2013, Guo et al. [4] used Computational Fluid Dynamics (CFD) and Finite Element Method (FEM) techniques to solve the hydroplaning effect. Their result showed that the impact of standing water depth on hydrodynamic pressure is very apparent on a vehicle traveling 90 km/hr.. Standing water at depths ranging from 5 mm to 8 mm present hydrodynamic pressure increases at the most apparent rate. It was suggested that a car should travel at mid or low speed (65 to 85 km/h) on wet roads. Nakajima et al. [5] used the CFD and FVM techniques to solve hydroplaning effects. They pointed out that simulations could clarify the water flow around the practical tread pattern. The simulation approach allowed developing new tire tread patterns within a short period based on the principle, "make the stream line smooth". In 2013, Croner et al. [6] published an article indicating that numerical CFD and experiments could demonstrate the wake conditions in a single water slick moving on the road. The simulation results indicated considerable changes in the contact area between the tires and the road surface. Kim et al. [7] recommended using a simplified model to conduct flow field analysis on tire tread patterns in contact with a road surface and then moving away from the road surface. Flow field analysis is then used to analyze the noise. The main object of this paper is therefore to study how to analyze tire hydroplaning effects on wet roads.

2. NUMERICAL SIMULATION

2.1 Model Structure

Many design parameters are necessary in producing high performance automobile tires. These parameters include the tire groove pattern, groove depth and width, tread geometric layout, rubber materials, noise level, rolling resistance, performance on both dry and wet roads. In order to investigate the hydroplaning effects this study designed five types of cases as listed in Table 1. Case 1 is simple design with only four tread ribs with 8mm and 10mm depth, without tread pattern design. The hydroplaning result is the reference base for the same layout design. Theoretically, a tire with a tread pattern will increase the hydroplaning effects but the pattern can improve manipulation performance, because the pattern can discharge more water through the tread grooves, improving he tire contact length and contact area. Case 2 is a pattern with groove depth of 8mm with the void pattern 31.7%. The groove depth for Case 3 is 10 mm with the void pattern the

same as case 2. We also know that the groove depth has a total depth limit. Therefore, in cases 4 and case 5 only the pattern void is changed from 35% to 38%. Large voids can improve the groove crawl water total volume.

2.2 Simulation model define

We used the 205/65R18 tire size, the most common passenger car tire in use to investigate tire hydroplaning with different tire tread designs. The calculation domain is shown in Figure 1. The mesh is rectangular with 905364 nodes. A supercomputer with 16 cores and 128G flash memory was used to calculate this problem. The simulation flow chart is shown in Figure 2. The first step is to draw the 3D geometry and modify the design pattern for mapping to our simulation requirements. The second step is outputting the CAD into the WRL format and checking if the geometry scale is reasonable. The next step is loading the WRL file into the CFD software and completing the simulation conditions. The final step is simulation and outputting the hydroplaning force between the water and tire surface.

2.3 Simulation Theory

2.3.1 Subgrid geometry resolution method

A goal of a proposed sub-grid geometry resolution method is to overcome the barrier between CAD systems and CFD code. Theoretically, common CAD systems can generate the description of object surface by set of plane facets. Using of this representation allows for CFD code to perceive geometry information from CAD. In this case the CFD code becomes compatible with other CAE systems based on finite element analysis. Let the adaptive locally refined grid (ALGR) has given in computational domain. At first stage of algorithm the facets intersecting the grid cell (Figure 3) are being found. Then the grid cell is disjoined into a set of finite volumes bounded by facets (or facet splinters) and cell faces (or face splinters). If the cell does not have any facets intersect with finite volume. Only allowable one situation is splinter facet can bounded finite volume. A finite volume is indexed by i and is designated as V_i. With the help of this technology, it can make program deal with the tire with complex thread pattern rolling in computational domain without problem of distortion of computational grid.

2.3.2 Governing equations solving

In this study, the water flow is inlet from input and contact with tires, therefore need consider governed by system of equations for incompressible fluid which includes continuity and Navier-Stokes equations. To consider the algorithm of the equations solving again write ones in Lagrange integral form for volume moved with fluid during intermitted time duration is:

$$\frac{\partial_p}{\partial_t} + \nabla \cdot (\rho V) = 0 \qquad (1)\ \frac{\partial_p V}{\partial_t} + \nabla \cdot (\rho V \otimes V) = -\nabla P + \nabla \cdot \hat{\tau}_{eff} + \rho F \qquad (2)$$

Equations (1) and (2) were used to solve the velocity and pressure of fluid with a decouple process called as *pressure-velocity split process* [8-10]. Here, $\hat{\tau}_{eff}$ is the effective shear stress tensor caused by viscosity of fluid. The turbulence of water flow around the rolling tire is also considered. The standard K-ε model, expressed as (3) and (4) is used to solve the turbulent energy and dissipation of fluid.

$$\frac{\partial(pk)}{\partial t} + \nabla \cdot (\rho V k) = \nabla\left(\left(\mu + \frac{\mu_t}{\sigma_k}\right)\nabla k\right) + \mu_t\left(G + \frac{\beta}{\mathrm{Pr}_t} g \cdot \nabla T\right) - \rho\varepsilon \qquad (3)$$

$$\frac{\partial(p\varepsilon)}{\partial t} + \nabla \cdot (\rho V \varepsilon) = \nabla\left(\left(\mu + \frac{\mu_t}{\sigma_\varepsilon}\right)\nabla\varepsilon\right) + C_1 \frac{\varepsilon}{k}\mu_t\left(G + \frac{\beta}{\mathrm{Pr}_t} g \cdot \nabla T\right) - C_2\rho\frac{\varepsilon^2}{k} \qquad (4)$$

The model parameters and the expression for generating term G can be rewritten as (5), (6), and (7):

$$G = D_{ij}\frac{\partial V_i}{\partial_{xj}} \qquad (5)$$

$$D_{ij} = S_{ij} - \frac{2}{3}\left(\nabla \cdot V + \frac{\rho k}{\mu_t}\right)\delta_{ij} \qquad (6)$$

$$S_{ij} = \frac{\partial V_i}{\partial x_j} + \frac{\partial V_j}{\partial x_i} \qquad (7)$$

The object of this study is to investigate the resistance force of a rolling tires caused by fluid-dynamic, we will introduced the similarity approach to experimentally measure the resistance of a tire rolling in an basin instead of wind tunnel for the validation of simulation. Therefore, the working fluid in this simulation is water, and heat transfer can be

neglected reasonably. The units and numerical settings are listed in Table 2. Equation (8) was used to solve the total pressure of fluid, and the total resistance force of a rolling tire is calculated by Equation (9)

$$P_{tot} = P + P_{hst} + \frac{1}{2}\rho|V_{abs}|^2 \tag{8}$$

$$F_{fluid} = \oint_s (P + P_{hst})ndS - \oint_s (\mu + \mu_t)\frac{\partial V}{\partial n}dS \tag{9}$$

3. SIMULATION RESULT

We used a smooth tire with four groves to investigate the basic hydroplaning effects on the tire layout. The original design is shown in Figure 4, with four grooves with two depths; 8mm and 10mm. The simulation result is shown in Figure 5. When the inlet water fill with the tire contact area and the tire has finished rolling one cycle. The stable hydroplaning effect for the 8mm groove is 2588(N) and 2336(N) for the 10mm groove. From this result we can see that the large groove depth can reduce the hydroplaning effect because greater groove volume means the crawl water volume is greater within the same time frame. Therefore, if the tire pattern design is not changed but the grooves are deeper, the hydroplaning effect can be reduced. In Figure 6 case 2 has 8mm depth and 31.7% pattern void as the other design for cases 3 and 4. Only the groove depth is changed from 8mm to 10mm and the pattern void width to 35% and 38%. The simulation result is shown in Figure 7. In this result the hydroplaning effects are 2394, 2491, 1646 and 1313(N). These simulations permit identifying when the groove depth presents no change (limit depth) and allows modifying the pattern void to reduce the hydroplaning effects. Large pattern voids can also help the tire crawl more water volume through the treads, reducing the water force feedback into the tire, maintaining more tire contact area with the road surface. Figure 8 shows the water splash simulation result in different cases. We can see that the water splash in the original design maintains more road contact than the other cases. In case 5 the water splash has some ruptures and does not remain intact, meaning the water force feedback into the tire is smaller. Therefore, this pattern void design can improve the hydroplaning effect.

4. CONCLUSION

In this paper presented CFD techniques used to simulate hydroplaning effects. The hydroplaning effects from different tire tread groove depths and pattern voids were analyzed. The simulation results demonstrate that tire tread grove depth modification is the most efficient way to reduce the hydroplaning effect. The tire tread geometry is the limiting factor because finite limits to the tire tread groove and pattern depth exist. Therefore, we can modify the pattern void to reduce the hydroplaning effect. Large tread pattern voids can also help the tire crawl more water volume through the tread, reducing the water force feedback into the tire, maintaining greater tire contact area with the road surface, improving tire safety performance on wet roads.

5. REFERENCES

[1] A. Lie, et al., "The effectiveness of ESC in reducing real life crashes and injuries," Traff. Inj. Prev. 7, 2006, pp.38–43.
[2] J. Strandroth, M. Rizzi, M. Olai, A. Lie, C. Tingvall, "The effects of studded tires on fatal crashes with passenger cars and the benefits of electronic stability control (ESC) in Swedish winter driving," Accident Analysis and Prevention, Vol.45, 2012, pp.50-60.
[3] M. Matilainen, A. Tuononen, "Tyre contact length on dry and wet road surfaces measured by three-axial accelerometer," Mechanical Systems and Signal Processing, Vol.52-53, 2015, pp.548-558.
[4] Xin-xin Guo, Chi Zhang, Bu-Xin Cui, Di Wang, James Tsai, "Analysis of Impact of Transverse Slope on Hydroplaning Risk Level," Procedia-Social and Behavioral Sciences, Vol.96, 2013, pp.2310-2319.
[5] Y. Nakajima, E. Seta, T. Kamegawa, H. Ogawa, "Hydroplaning Analysis by FEM and FVM: Effect of Tire Rolling and Tire Pattern on Hydroplaning," FISITA World Automotive Congress, 2000, F2000G382.
[6] E. Croner, H. Bézard, C. Sicot, G. Mothay, "Aerodynamic characterization of the wake of an isolated rolling wheel," *International Journal of Heat and Fluid Flow*, Vol.43, 2013, pp.233-243.
[7] S. Kim, W. Jeong, Y. Park, S. Lee, "Prediction method for tire air-pumping noise using a hybrid technique," *J. Acoust. Soc. Am*, Vol.119, 2006, pp. 3799-3812.
[8] Aksenov, A.A., Gudzovsky, A.V., "The software FlowVision for study of air flows, heat and mass transfer by numerical methods," *Third Forum of Association of Engineers for Heating, Ventilation, Air-Conditioning, Heat Supply and Building Thermal Physics*, Vol.31-35, 1993, pp.22-25.
[9] Aksenov A.A., Dyadkin A.A., Gudzovsky A.V., "Numerical Simulation of Car Tire Aquaplaning,"*Computational Fluid Dynamics*, 1996, pp. 815-820.
[10] CAPVIDIA FlowVision HPC version 3.08.05, 2014 user manual.

APPENDIX

Table 1 Simulation items for different tire designs

Items	Case1	Case2	Case3	Case4	Case5
Patten	No	Yes	Yes	Yes	Yes
Depth(mm)	8 / 10	8	10	10	10
Void (%)	----	31.7	31.7	35	38

Table 2 Units and numerical settings. [10]

Notation	Physical quantity	Dimension	Notation	Physical quantity	Dimension
C_p	specific heat=1008.69	$m^2s^{-2}K^{-1}$	**Q**	sum of the energy of different nature	m^2s^{-2}
F	acceleration of external volume face	ms^{-2}	R_A	universal gas constant= 8.31441	$Jmole^{-1}K^{-1}$
G	gravity acceleration	ms^{-2}	T_{tot}	total temperature	°K
H	total enthalpy	m^2s^{-2}	T_{ref}	reference temperature = 273	°K
K	turbulent energy	m^2s^{-2}	T_{abs}	absolute temperature	°K
L	characteristic length	m	T^n	temperature value at time layer n	°K
M	molar mass=0.02884	$kgmile^{-1}$	**μ**	molecular dynamic viscosity	$kgm^{-1}s^{-1}$
P	relative pressure	Pa	μ_t	turbulent dynamic viscosity	$kgm^{-1}s^{-1}$
P_{ref}	reference pressure= 101000	Pa	***V***	relative velocity	m/s
P_{hst}	hydrostatic pressure	Pa	V^n	velocity value at time layer n	m/s
P_{abs}	absolute pressure	Pa	ρ^n	density value at time layer n	$kg\ m^{-3}$
P_{tot}	total pressure	Pa	ρ^{n+1}	density value at time layer n+1	$kg\ m^{-3}$
Pr_t	turbulent prandtl number	----	**ε**	dissipation rate of turbulent energy	m^2s^{-2}
P^n	pressure value at time layer n	Pa	**β**	coefficient of thermal expansion	$°K^{-1}$
P^{n+1}	pressure value at time layer n+1	Pa	∂T	relative local specific	Kgs^{-2}

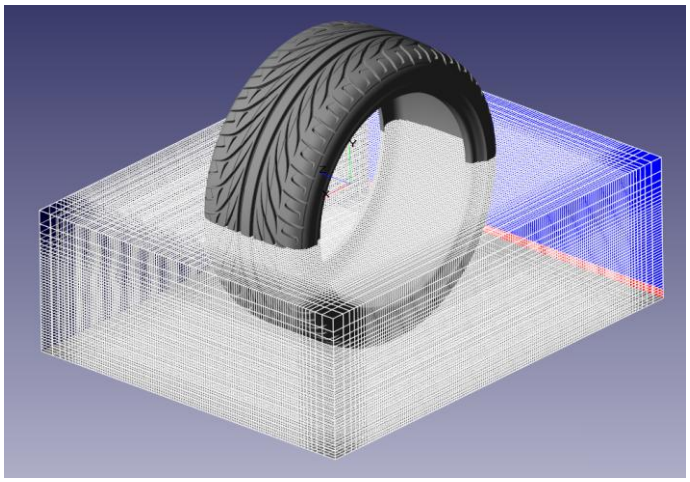

Figure 1 Mesh defined for calculation domain.

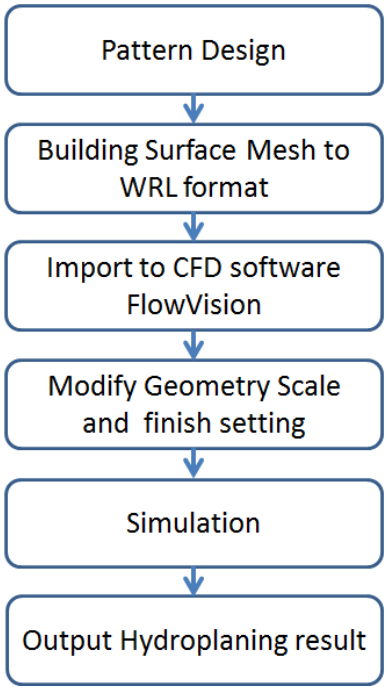

Figure 2 Sketch of the simulation step.

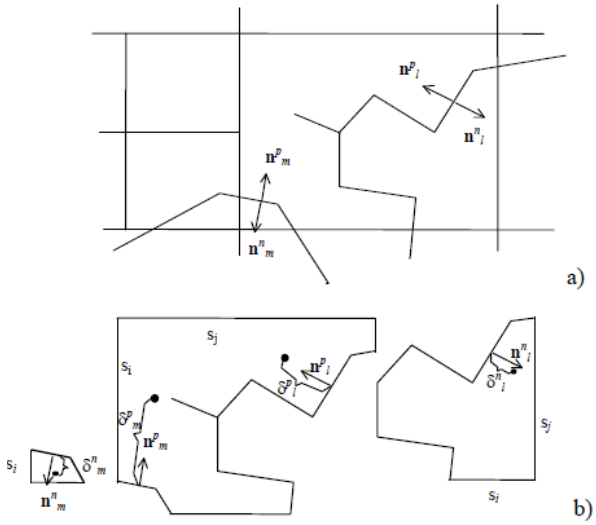

Figure 3 Sub-grid geometry resolution; (a) finding of facets intersected ALGR cell (b) disjoining of cell into finite volumes

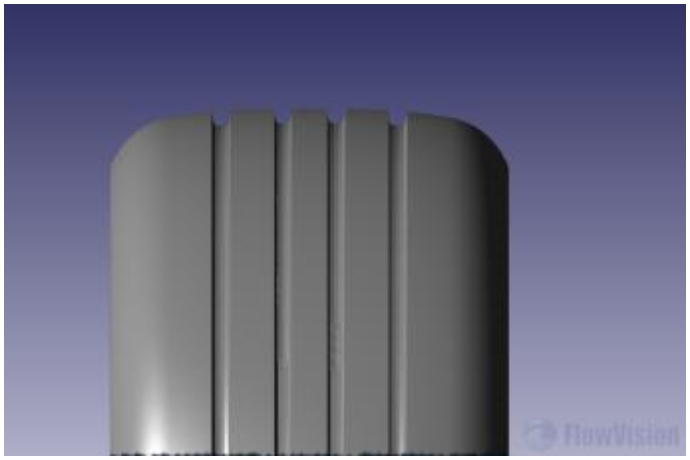

Figure 4 Picture of the tire design: Case 1

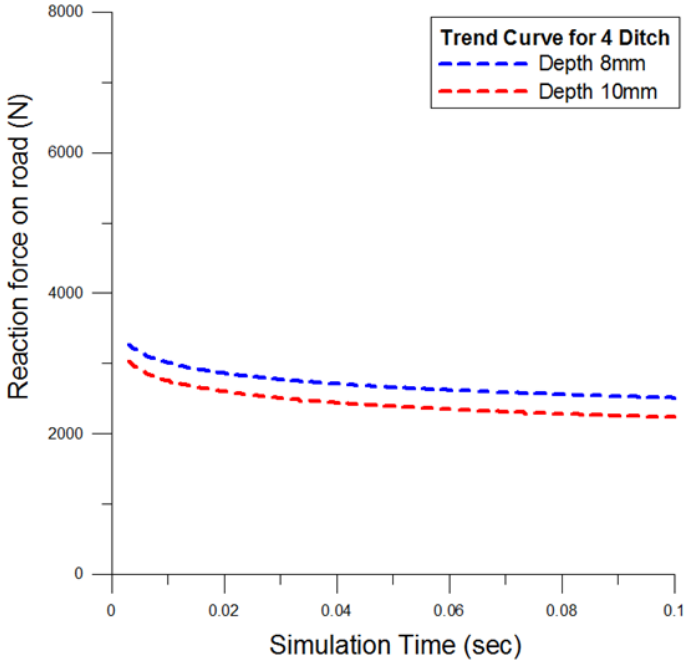

Figure 5 Hydroplaning result for Case1

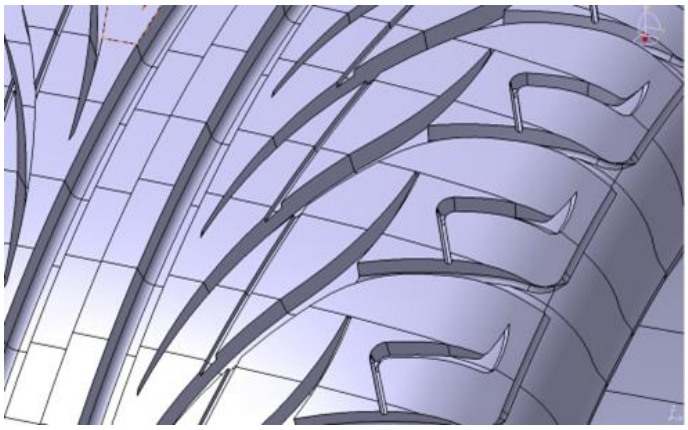

Figure 6 Picture of the tire design: Case2

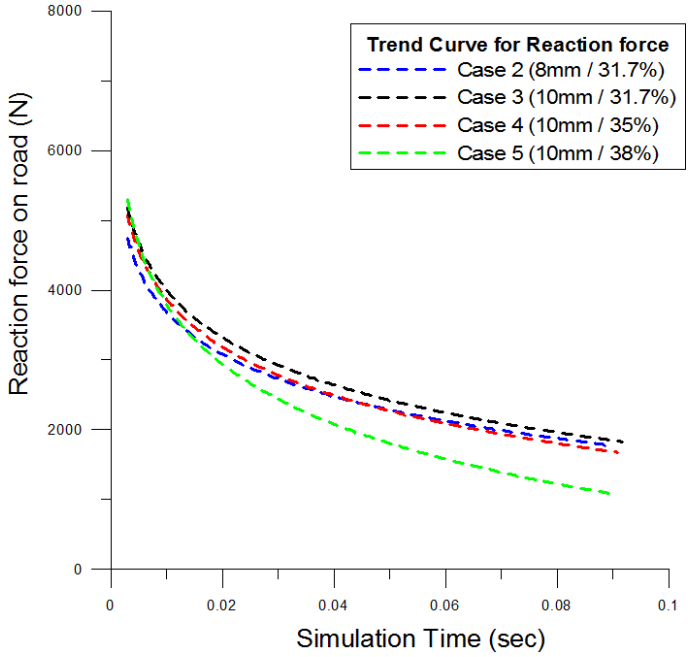

Figure 7 Hydroplaning result for Case2 to Case5

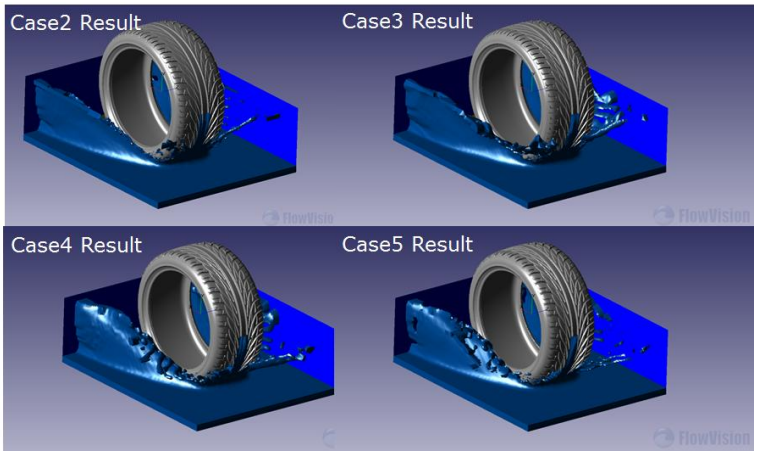

Figure 8 Simulation result of the water splash contour.